2019

Analytical expressions for characterising voltage dips and phase-angle jumps in electricity networks

Most Begum
University of Wollongong

Mollah R. Alam
University of Wollongong, mra497@uowmail.edu.au

Kashem M. Muttaqi
University of Wollongong, kashem@uow.edu.au

Analytical expressions for characterising voltage dips and phase-angle jumps in electricity networks

Abstract

Voltage dips/sags are one of the major concerns for electricity consumers as well as utility service providers. Therefore, the characterisation of voltage dips/sags is required. This study presents a set of mathematical expressions for characterising different types of voltage dips/sags and their associated phase-angle jumps, which are typically found due to faults and/or disturbances in electricity networks. The expressions are derived analytically from the model of the power network containing generators, transmission and/or distribution lines, transformers etc. Four types of voltage dips, namely, A, B, E, and G, which are associated with four major types of faults including balanced three-phase faults, single line-to-ground, double lineto- ground, and line-to-line faults, are considered to derive the analytical expressions. Dynamic simulation results, using a test distribution system, approve the validity as well as the accuracy of the developed expressions. The influence of fault-types and fault-locations is investigated from the mathematical expressions; further, validation is conducted through a simulation study. The analytical expressions, presented in this study, are a valuable tool in the planning stage since the expressions can be employed to characterise during-fault voltage dips at different buses in electricity network without conducting a large number of repeated dynamic simulations.

Disciplines

Engineering | Science and Technology Studies

Publication Details

M. Tasneem Ara. Begum, M. Rezaul. Alam & K. M. Muttaqi, "Analytical expressions for characterising voltage dips and phase-angle jumps in electricity networks," IET Generation, Transmission and Distribution, vol. 13, (1) pp. 116-126, 2019.

Analytical Expressions for Characterising Voltage Dips and Phase-Angle Jumps in Electricity Networks

Most. T. A. Begum[1], M. R. Alam[2*], Kashem M. Muttaqi [3]

[1]School of Electrical, Computer & Telecommunications Engineering, University of Wollongong, NSW 2522, Australia

[2]School of Electrical, Computer & Telecommunications Engineering, University of Wollongong, NSW 2522, Australia

[3]School of Electrical, Computer & Telecommunications Engineering, University of Wollongong, NSW 2522, Australia

[*]mra497@uowmail.edu.au

Abstract:Voltage dips/sags are one of the major concerns for electricity consumers as well as utility service providers. Therefore, characterisation of voltage dips/sags is required. This article presents a set of mathematical expressions for characterising different types of voltage dips/sags and their associated phase-angle jumps, which are typically found due to faults and/or disturbances in electricity networks. The expressions are derived analytically from the model of power network containing generators, transmission and/or distribution lines, transformers, etc. Four types of voltage dips, namely, A, B, E and G, which are associated with four major types of faults including balanced 3-phase faults, single line-to-ground (SLG), double line-to-ground, and line-to-line faults, are considered to derive the analytical expressions. Dynamic simulation results, using a test distribution system, approve the validity as well as accuracy of the developed expressions. The influence of fault-types and fault-locations is investigated from the mathematical expressions; further validation is conducted through simulation study. The analytical expressions, presented in this paper, are a valuable tool in the planning stage, since the expressions can be employed to characterise during-fault voltage dips at different buses in electricity network without conducting a large number of repeated dynamic simulations.

1. Introduction

Power quality (PQ) is a concept, which has been evolved through multi-dimensional aspects because of technological advancement and consumers' awareness of quality services. Formerly, reliability, i.e., the continuity of electricity supply, was the only PQ concern. Now, PQ includes several issues, e.g., voltage sags/dips, temporary and/or permanent fluctuations, interruptions and harmonics of different orders, etc. [1]. The increased utilization of power electronic devices in electricity networks accelerates the PQ degradation, thereby requiring extra attention from the power sector agents [2].

Voltage dip/sag is regarded as a significant PQ issue similar to long and short interruptions in the electricity supply [3-4]. They are usually defined as the reduction of root-mean-square (rms) voltage for a short-duration; reduction of voltage is typically triggered by switching of loads, motors, generators, transformer energisation and short circuits in power networks [5]. Despite the comprehensive efforts practiced by the utilities and customers to improve the reliability of electricity networks, several challenges still exist in order to control the external factors causing voltage sags/dips.

Voltage dips have a significant economic impact in power systems [6-7]. The economic losses encompass temporary or permanent damage to electrical equipment, delay in product delivery, and hence, lead to customer dissatisfaction [8]. The total costs, which are associated with the power system disturbances, can be estimated by following the guidelines recommended in IEEE Standard 1346-1998 [9]. To this end, the authors of [10] proposed a probabilistic model to evaluate the economic damages due to voltage dips and interruptions. Therefore, detection, evaluation and classification of voltage dips are essential for testing of equipment, monitoring of power quality, analysis of voltage dips, and thus mitigation of disturbances causing voltage dips.

Most electrical/electronic equipment is only concerned with voltage dip-magnitude. Hence, voltage dip-magnitude is emphasized in most of the developed methods in literatures [11-12]. However, faults (symmetrical and unsymmetrical) in a power system may change magnitude as well as phase-angle of the voltage. Therefore, power-electronics equipment, whose firing instants are triggered by the phase-angle information, may have adverse impact [4], [13-14]. To this end, several methods are reported in various research works for classification and characterisation of voltage dips[15-21].In [22], fault-types and fault-locations, which trigger voltage sags and swells, are investigated by capturing fault records. However, this paper proposes an analytical approach for assessment of voltage sags caused by balanced as well as unbalanced faults. The proposed methoddoes not require any fault or voltage dips/swells records as needed by other reported methods. The proposed analytical approach considers the voltage dips, which are triggered by short-circuit faults along the feeders, and formulates the expressions of voltage dips and phase-angle jumps. A simple *n*-bus radial system has been employed for developing the analytical expressions of voltage dips and phase-angle jumps associated with four types of dips (A. B, E and G) as proposed in [4].

The remaining part of the paper is structured as follows. Section 2 describes the systematic procedure for developing the analytical expressions of voltage dips due to balanced and unbalanced faults. An illustrative example is presented in section 3 in order to validate the developed expressions. Section 4 highlights the severity of voltage dips for different fault-types, fault-location and different monitoring points. Section 5 presents the concluding remarks.

2. Voltage Dips and Phase Angle Jumps

Voltage dips may occur from motor-starting, transformer energising, and short-circuits in the transmission and/or distribution system. In this section, voltage dips/sags initiated by short-circuits are analysed. Firstly, an analytical expression of voltage is presented for a distribution network, where voltage dip occurs due to fault. To this end, the general expressions of four types of voltage dips (A, B, E and G) are developed and presented in the following section.

In order to determine the voltages at different buses of a test network, the distribution network model of Fig. 1 is considered. This model comprises source impedance ($\boldsymbol{Z}_s$) at the point of common coupling (PCC). The source voltage $\boldsymbol{E}_s$ and impedance $\boldsymbol{Z}_s$ are regarded as Thévenin equivalent of the upstream side. A total of n number of buses is shown in the model, where a fault (with fault impedance $\boldsymbol{Z}_f$) occurs at bus x. In this model, load currents are assumed negligible during fault (since fault currents are typically very high in comparison to load current). Note that firstly, the general expressions of voltage dips associated with different types of faults and their corresponding types of dips are developed. Then, the expressions of phase-angle jump during fault are presented.

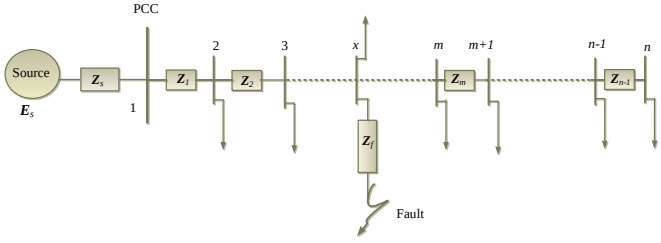

Fig. 1. *Single line diagram of a typical distribution network.*

To formulate the general expressions of voltages during different types of faults, in Section 2.1, sequence-network diagram is formed considering the positive, negative and zero sequence impedance of the network. In Section 2.2, the 3-phase voltages during-fault (or the during-fault voltage) at a monitoring bus m are determined. Then, in Section 2.3, taking four types of voltage dips into account, voltage-dip d_v is expressed as a function of sequence-impedance component of the network. Moreover, phase-angle jumps associated with different dip-types are developed and presented subsequently.

2.1. Sequence Network Diagrams for different types of Faults

Considering the test system of Fig. 1, voltage-current relationship can be given in terms of bus admittance matrix

$$\begin{bmatrix} \boldsymbol{I}_1 \\ \boldsymbol{I}_2 \\ \boldsymbol{I}_x \\ \dots \\ \boldsymbol{I}_m \\ \dots \\ \boldsymbol{I}_n \end{bmatrix} = \begin{bmatrix} \boldsymbol{Y}_{11} & \boldsymbol{Y}_{12} \dots \boldsymbol{Y}_{1x} \dots \boldsymbol{Y}_{1m} \dots \boldsymbol{Y}_{1n} \\ \boldsymbol{Y}_{21} & \boldsymbol{Y}_{22} \dots \boldsymbol{Y}_{2x} \dots \boldsymbol{Y}_{2m} \dots \boldsymbol{Y}_{2n} \\ \dots \\ \boldsymbol{Y}_{x1} & \boldsymbol{Y}_{x2} \dots \boldsymbol{Y}_{xx} \dots \boldsymbol{Y}_{xm} \dots \boldsymbol{Y}_{xn} \\ \dots \\ \boldsymbol{Y}_{m1} & \boldsymbol{Y}_{m2} \dots \boldsymbol{Y}_{mx} \dots \boldsymbol{Y}_{mm} \dots \boldsymbol{Y}_{mn} \\ \dots \\ \boldsymbol{Y}_{n1} & \boldsymbol{Y}_{n2} \dots \boldsymbol{Y}_{nx} \dots \boldsymbol{Y}_{nm} \dots \boldsymbol{Y}_{nn} \end{bmatrix} \begin{bmatrix} \boldsymbol{V}_1 \\ \boldsymbol{V}_2 \\ \boldsymbol{V}_x \\ \dots \\ \boldsymbol{V}_m \\ \dots \\ \boldsymbol{V}_n \end{bmatrix} \quad \textbf{(1a)}$$

Or

$$[\boldsymbol{I}] = [\boldsymbol{Y}_{BUS}][\boldsymbol{V}] \quad (1b)$$

Re-arranging Eq. (1b) yields

$$[\boldsymbol{V}] = [\boldsymbol{Y}_{BUS}]^{-1}[\boldsymbol{I}] = [\boldsymbol{Z}][\boldsymbol{I}] \quad (2)$$

where $\boldsymbol{Z}$ refers to the bus impedance matrix $\left([\boldsymbol{Z}] = [\boldsymbol{Y}_{BUS}]^{-1}\right)$ and the elements of $\boldsymbol{Z}$ are divided into two parts: driving point impedance and transfer impedance, which can be presented as below:

$$Z_{kl} = \begin{cases} \text{driving point impedance} & \text{when} k = l \\ \text{transfer impedance} & \text{when} k \neq l \end{cases}$$

The driving point impedance of a bus/node is equal to the Thévenin equivalent impedance of the network observed from that bus/node. Therefore, the driving point impedance or the diagonal elements of $\boldsymbol{Z}$ is applied to calculate the short-circuit current due to faults at different buses. In short-circuit studies, symmetrical components are assumed independent. In other words, assuming the network as symmetrical, where an unsymmetrical fault takes place, the three sequence components, i.e., positive, negative and zero sequence components, are independent of each other.

For the test network of Fig. 1, the positive, negative and zero sequence impedance matrix are built to develop the sequence network diagram associated with balanced and unbalanced faults. Therefore, three single-phase sequence network diagrams are required for individual consideration. These sequence diagrams are single-phase models of the power system and the impedance matrix can be used to model them. Using the method proposed in [23-24] the three-sequence bus impedance matrix for the network can be easily obtained.

In order to build the sequence impedance matrix, the sequence impedance (positive, negative and zero sequence) encountered by the currents is investigated. It reveals that sequence currents depend on power system equipment, such as, transmission/distribution line, transformer, generator, etc. Both positive and negative sequence impedance of non-rotating apparatus, e.g., transmission/distribution line, is same. However, zero sequence impedance of overhead line usually lies between two to six times of positive sequence impedance, and it depends on grounding wires, tower footing resistance, etc. The leakage impedance of transformers represent the positive and negative sequence impedance, whereas zero sequence impedance of transformers varies from open circuit to a low value based on the connection of transformer winding, the core construction and method of neutral grounding [25]. For evaluating the synchronous generator's performance, the positive sequence synchronous reactance, X_d, is used in steady state analysis, whereas subtransient reactance $\left(X_d''\right)$ and transient reactance $\left(X_d'\right)$ is

used in transient study. Negative and zero sequence impedance of synchronous machine are provided by the manufactures, based on their test results.

The above discussion concludes that the positive-sequence network is almost equal to the negative-sequence with two exceptions: a source is absent in the negative-sequence network and the reactance of the generator due to negative-sequence may be different from the positive one. The structure of positive-sequence impedance matrix $(\boldsymbol{Z}^{P})$ is similar to the negative one $(\boldsymbol{Z}^{N})$, but a small numerical difference may be found which is negligible. The zero-sequence impedance matrix is quite different from negative and positive ones. It has no voltage source and has discontinuities due to transformer winding connections, and the impedance values are different from positive ones.

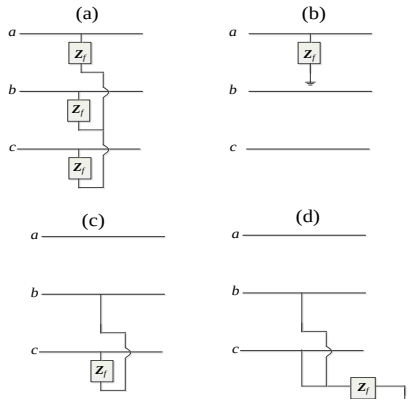

Fig. 2. *Hypothetical connection diagrams for* ***(a)*** *3-phase symmetrical fault,* ***(b)*** *single line-to-ground (SLG) fault,* ***(c)*** *phase-to-phase fault, and* ***(d)*** *double line-to-ground fault, through fault impedance.*

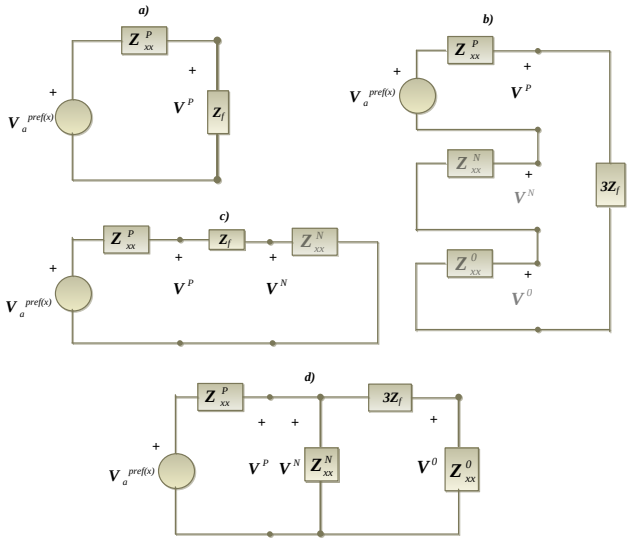

Fig. 3. *Sequence network diagrams for (a) 3-phase symmetrical fault, (b) single line-to-ground (SLG) fault, (c) phase-to-phase fault, and (d) double line-to-ground fault.*

Four major types of short-circuit faults are normally found in power systems, they are: a) balanced three-phase fault, b) single-phase/line to ground fault, c) phase-to-phase fault, and d) double line-to-ground fault. Fault a) is known as symmetrical or balanced fault whereas faults b), c) and d) are regarded as unbalanced faults. The connection diagrams of the hypothetical stubs for these four types of faults through a fault-impedance $\boldsymbol{Z}_f$ are shown in Fig. 2.

Note thatin this work, the steady-state values of positive, negative and zero sequence impedance of the investigated network components, for example, transformers, line, generators, etc., are obtained from the data provided by the network operator.Now, considering a fault at bus *x* (with fault impedance $\boldsymbol{Z}_f$) of Fig. 1, the sequence network diagrams associated with the four types of faults are illustrated in Fig. 3. It should be noted that in Fig. 3, the superscripts *0, P* and *N* over the variables indicate the zero, positive and negative sequence components and $\boldsymbol{V}_a^{pref(x)}$ indicates *a*-phase voltage at faulted bus *x* prior to the fault.

2.2. Expression of Phase-voltages during different types of Faults

Development of the expressions for 3-phase voltages during balanced and unbalanced dip (associated with balanced and unbalanced faults) is presented below.

*2.2.1 Balanced Voltage Dip:*Balanced dips are caused by three-phase faults. Considering a three-phase fault at bus *x* of Fig. 1 (with fault impedance $\boldsymbol{Z}_f$), voltage at node *m* (monitoring bus) during the fault is given by

$$\boldsymbol{V}^{mx} = \boldsymbol{V}^{pref(m)} + \Delta\boldsymbol{V}^{mx} \tag{3}$$

where $\boldsymbol{V}^{mx}$ = Voltage at monitoring bus *m* due to 3-phase fault at bus/node *x*,

$\boldsymbol{V}^{pref(m)}$ = Pre-fault voltage at monitoring bus *m*, and

$\Delta\boldsymbol{V}^{mx}$ = Change in voltage at monitoring bus *m* due to 3-phase fault at bus/node *x*.

Equation (3) shows that the voltage during the fault is equal to the pre-fault voltage at the monitoring bus plus the change of voltage due to the fault.Now, during three-phase short-circuit at *x*, the current "injected" into *x* is given by (4), where $\boldsymbol{V}^{pref(x)}$ is the pre-fault voltage at bus *x*, $\boldsymbol{Z}_{xx}$ is the Thévenin impedance or the impedance seen from the faulted bus *x* into the network, and the minus sign is considered due to the direction of current. Only positive-sequence values are required to perform the calculations.

$$\boldsymbol{I}_x = -\frac{\boldsymbol{V}^{pref(x)}}{\boldsymbol{Z}_{xx} + \boldsymbol{Z}_f} \tag{4}$$

Once the "injected" current is known, the voltage-change at any bus *m* can be calculated using the transfer impedance between bus *m* and node *x*, denoted as $\boldsymbol{Z}_{mx}$. Thus, change in voltage is given by

$$\Delta\boldsymbol{V}^{mx} = -\boldsymbol{Z}_{mx}\frac{\boldsymbol{V}^{pref(x)}}{\boldsymbol{Z}_{xx} + \boldsymbol{Z}_f} \tag{5}$$

From (3) and (5), the during-fault voltage at bus *m*, due to 3-phase fault at *x*, is obtained as

$$\boldsymbol{V}^{mx} = \boldsymbol{V}^{pref(m)} - \boldsymbol{Z}_{mx}\frac{\boldsymbol{V}^{pref(x)}}{\boldsymbol{Z}_{xx} + \boldsymbol{Z}_f} \tag{6}$$

Equation (6) shows that the voltage-change at bus *m* due to a 3-phase fault at node *x* is given by the ratio of the transfer impedance to the driving point impedance at the faulted bus/node.

*2.2.2 Unbalanced Voltage Dip:*Symmetrical components are used for the analysis of unbalanced voltage dips which are caused by unsymmetrical faults. As the sequence components are independent in symmetrical systems, the during-fault voltage for each sequence components can be determined by using (3). Before the fault, only a positive-sequence component $\left(\boldsymbol{V}^{P,pref}\right)$ exists in the node voltages; therefore, pre-fault voltage of negative and zero sequences are zero. The during-fault sequence voltages are given by

$$\boldsymbol{V}^{\boldsymbol{P}} = \boldsymbol{V}^{P,pref} + \Delta \boldsymbol{V}^{P} \tag{7a}$$

$$\boldsymbol{V}^{\boldsymbol{N}} = 0 + \Delta \boldsymbol{V}^{N} \tag{7b}$$

$$\boldsymbol{V}^{0} = 0 + \Delta \boldsymbol{V}^{0} \tag{7c}$$

Considering phase-*a* as the symmetrical phase, the phase voltages can be obtained by applying the symmetrical components transformation as presented below.

$$\begin{bmatrix} \boldsymbol{V}_a \\ \boldsymbol{V}_b \\ \boldsymbol{V}_c \end{bmatrix} = \begin{bmatrix} 1 & 1 & 1 \\ 1 & a^2 & a \\ 1 & a & a^2 \end{bmatrix} \begin{bmatrix} \boldsymbol{V}^{0} \\ \boldsymbol{V}^{\boldsymbol{P}} \\ \boldsymbol{V}^{\boldsymbol{N}} \end{bmatrix} \tag{8}$$

From (7) and (8), the phase-voltages can be presented as

$$\boldsymbol{V}_a = \boldsymbol{V}^{P,pref} + \Delta \boldsymbol{V}^{P} + \Delta \boldsymbol{V}^{N} + \Delta \boldsymbol{V}^{0} \tag{9a}$$

$$\boldsymbol{V}_b = a^2 \boldsymbol{V}^{P,pref} + a^2 \Delta \boldsymbol{V}^{P} + a \Delta \boldsymbol{V}^{N} + \Delta \boldsymbol{V}^{0} \tag{9b}$$

$$\boldsymbol{V}_c = a \boldsymbol{V}^{P,pref} + a \Delta \boldsymbol{V}^{P} + a^2 \Delta \boldsymbol{V}^{N} + \Delta \boldsymbol{V}^{0} \tag{9c}$$

2.2.2.1Unbalanced Voltage Dip due to Single-Line-to-Ground (SLG) Fault:As shown in Fig. 3(b), due to single-phase or single line-to-ground (SLG) fault at bus *x*, the current injected into the positive, negative and zero sequence networks, is given by

$$\boldsymbol{I}_x^{P} = -\frac{\boldsymbol{V}_a^{pref(x)}}{\boldsymbol{Z}_{xx}^{P} + \boldsymbol{Z}_{xx}^{N} + \boldsymbol{Z}_{xx}^{0} + 3\boldsymbol{Z}_f}; \boldsymbol{I}_x^{P} = \boldsymbol{I}_x^{N} = \boldsymbol{I}_x^{0} \tag{10}$$

Now, the sequence voltage-changes at bus *m* due to fault at bus *x* are given by

$$\Delta \boldsymbol{V}^{P,mx} = -\boldsymbol{Z}_{mx}^{P} \frac{\boldsymbol{V}_a^{pref(x)}}{\boldsymbol{Z}_{xx}^{P} + \boldsymbol{Z}_{xx}^{N} + \boldsymbol{Z}_{xx}^{0} + 3\boldsymbol{Z}_f} \tag{11a}$$

$$\Delta \boldsymbol{V}^{N,mx} = -\boldsymbol{Z}_{mx}^{N} \frac{\boldsymbol{V}_a^{pref(x)}}{\boldsymbol{Z}_{xx}^{P} + \boldsymbol{Z}_{xx}^{N} + \boldsymbol{Z}_{xx}^{0} + 3\boldsymbol{Z}_f} \tag{11b}$$

$$\Delta \boldsymbol{V}^{0,mx} = -\boldsymbol{Z}_{mx}^{0} \frac{\boldsymbol{V}_a^{pref(x)}}{\boldsymbol{Z}_{xx}^{P} + \boldsymbol{Z}_{xx}^{N} + \boldsymbol{Z}_{xx}^{0} + 3\boldsymbol{Z}_f} \tag{11c}$$

The during-fault sequence voltages at node *m* are given by

$$\boldsymbol{V}^{P,mx} = \boldsymbol{V}_a^{pref(m)} - \boldsymbol{Z}_{mx}^{P} \frac{\boldsymbol{V}_a^{pref(x)}}{\boldsymbol{Z}_{xx}^{P} + \boldsymbol{Z}_{xx}^{N} + \boldsymbol{Z}_{xx}^{0} + 3\boldsymbol{Z}_f} \tag{12a}$$

$$\boldsymbol{V}^{N,mx} = -\boldsymbol{Z}_{mx}^{N} \frac{\boldsymbol{V}_a^{pref(x)}}{\boldsymbol{Z}_{xx}^{P} + \boldsymbol{Z}_{xx}^{N} + \boldsymbol{Z}_{xx}^{0} + 3\boldsymbol{Z}_f} \tag{12b}$$

$$\boldsymbol{V}^{0,mx} = -\boldsymbol{Z}_{mx}^{0} \frac{\boldsymbol{V}_a^{pref(x)}}{\boldsymbol{Z}_{xx}^{P} + \boldsymbol{Z}_{xx}^{N} + \boldsymbol{Z}_{xx}^{0} + 3\boldsymbol{Z}_f} \tag{12c}$$

Transforming back to phase components, the phase-voltages due to SLG faults are obtained as follows,

$$\boldsymbol{V}_a^{mx} = \boldsymbol{V}_a^{pref(m)} - \left(\boldsymbol{Z}_{mx}^{P} + \boldsymbol{Z}_{mx}^{N} + \boldsymbol{Z}_{mx}^{0}\right) \frac{\boldsymbol{V}_a^{pref(x)}}{\left(\boldsymbol{Z}_{xx}^{P} + \boldsymbol{Z}_{xx}^{N} + \boldsymbol{Z}_{xx}^{0} + 3\boldsymbol{Z}_f\right)} \tag{13a}$$

$$\boldsymbol{V}_b^{mx} = a^2 \boldsymbol{V}_a^{pref(m)} - \left(a^2 \boldsymbol{Z}_{mx}^{P} + a \boldsymbol{Z}_{mx}^{N} + \boldsymbol{Z}_{mx}^{0}\right) \frac{\boldsymbol{V}_a^{pref(x)}}{\left(\boldsymbol{Z}_{xx}^{P} + \boldsymbol{Z}_{xx}^{N} + \boldsymbol{Z}_{xx}^{0} + 3\boldsymbol{Z}_f\right)} \tag{13b}$$

$$\boldsymbol{V}_c^{mx} = a \boldsymbol{V}_a^{pref(m)} - \left(a \boldsymbol{Z}_{mx}^{P} + a^2 \boldsymbol{Z}_{mx}^{N} + \boldsymbol{Z}_{mx}^{0}\right) \frac{\boldsymbol{V}_a^{pref(x)}}{\left(\boldsymbol{Z}_{xx}^{P} + \boldsymbol{Z}_{xx}^{N} + \boldsymbol{Z}_{xx}^{0} + 3\boldsymbol{Z}_f\right)} \tag{13c}$$

2.2.2.2Unbalanced Voltage Dip due to Phase-to-Phase Fault:In the analysis of phase-to-phase fault, only the negative and positive sequence networks participate. As shown in Fig. 3(c), the positive- and negative-sequence current at the fault location is equal in magnitude, but the direction is opposite. Equation (14) gives the injected currents in the sequence networks.

$$\boldsymbol{I}_x^{P} = -\frac{\boldsymbol{V}_a^{pref(x)}}{\boldsymbol{Z}_{xx}^{P} + \boldsymbol{Z}_{xx}^{N} + \boldsymbol{Z}_f}; \boldsymbol{I}_x^{P} = -\boldsymbol{I}_x^{N} \tag{14}$$

The change of sequence voltages are given by

$$\Delta \boldsymbol{V}^{P,mx} = -\boldsymbol{Z}_{mx}^{P} \frac{\boldsymbol{V}_a^{pref(x)}}{\boldsymbol{Z}_{xx}^{P} + \boldsymbol{Z}_{xx}^{N} + \boldsymbol{Z}_f} \tag{15a}$$

$$\Delta \boldsymbol{V}^{N,mx} = \boldsymbol{Z}_{mx}^{N} \frac{\boldsymbol{V}_a^{pref(x)}}{\boldsymbol{Z}_{xx}^{P} + \boldsymbol{Z}_{xx}^{N} + \boldsymbol{Z}_f} \tag{15b}$$

Moreover, the change of zero-sequence voltage is zero. Thus, the phase-voltages are obtained by adding the pre-fault voltage to (15a) and then, performing the transformation of sequence components to phase components. This yields the phase-voltages, at bus *m* due to phase-to-phase faults at bus *x*, as given below

$$\boldsymbol{V}_a^{mx} = \boldsymbol{V}_a^{pref(m)} + \left(\boldsymbol{Z}_{mx}^{N} - \boldsymbol{Z}_{mx}^{P}\right) \frac{\boldsymbol{V}_a^{pref(x)}}{\left(\boldsymbol{Z}_{xx}^{P} + \boldsymbol{Z}_{xx}^{N} + \boldsymbol{Z}_f\right)} \tag{16a}$$

$$\boldsymbol{V}_b^{mx} = a^2 \boldsymbol{V}_a^{pref(m)} + \left(a \boldsymbol{Z}_{mx}^{N} - a^2 \boldsymbol{Z}_{mx}^{P}\right) \frac{\boldsymbol{V}_a^{pref(x)}}{\left(\boldsymbol{Z}_{xx}^{P} + \boldsymbol{Z}_{xx}^{N} + \boldsymbol{Z}_f\right)} \tag{16b}$$

$$\boldsymbol{V}_c^{mx} = a \boldsymbol{V}_a^{pref(m)} + \left(a^2 \boldsymbol{Z}_{mx}^{N} - a \boldsymbol{Z}_{mx}^{P}\right) \frac{\boldsymbol{V}_a^{pref(x)}}{\left(\boldsymbol{Z}_{xx}^{P} + \boldsymbol{Z}_{xx}^{N} + \boldsymbol{Z}_f\right)} \tag{16c}$$

2.2.2.3Unbalanced Voltage Dip due to Double-Phase-to-Ground Fault:Following the diagram shown in Fig. 3(d), the fault current due to two-phase-to-ground fault can be easily derived. The three sequence currents are different as the sequence networks are connected in parallel. Thus, the injected currents in the sequence networks are given by

$$\boldsymbol{I}_x^P = -\frac{\boldsymbol{V}_a^{pref(x)}}{\boldsymbol{Z}_{xx}^P + \dfrac{\boldsymbol{Z}_{xx}^N\left(\boldsymbol{Z}_{xx}^0 + 3\boldsymbol{Z}_f\right)}{\boldsymbol{Z}_{xx}^N + \boldsymbol{Z}_{xx}^0 + 3\boldsymbol{Z}_f}} \quad (17a)$$

$$= -\frac{\boldsymbol{V}_a^{pref(x)}\left(\boldsymbol{Z}_{xx}^N + \boldsymbol{Z}_{xx}^0 + 3\boldsymbol{Z}_f\right)}{\boldsymbol{Z}_{xx}^P\boldsymbol{Z}_{xx}^N + \boldsymbol{Z}_{xx}^P\left(\boldsymbol{Z}_{xx}^0 + 3\boldsymbol{Z}_f\right) + \boldsymbol{Z}_{xx}^N\left(\boldsymbol{Z}_{xx}^0 + 3\boldsymbol{Z}_f\right)}$$

$$\boldsymbol{I}_x^N = \frac{\boldsymbol{V}_a^{pref(x)}\left(\boldsymbol{Z}_{xx}^0 + 3\boldsymbol{Z}_f\right)}{\boldsymbol{Z}_{xx}^P\boldsymbol{Z}_{xx}^N + \boldsymbol{Z}_{xx}^P\left(\boldsymbol{Z}_{xx}^0 + 3\boldsymbol{Z}_f\right) + \boldsymbol{Z}_{xx}^N\left(\boldsymbol{Z}_{xx}^0 + 3\boldsymbol{Z}_f\right)} \quad (17b)$$

$$\boldsymbol{I}_x^0 = \frac{\boldsymbol{V}_a^{pref(x)}\boldsymbol{Z}_{xx}^N}{\boldsymbol{Z}_{xx}^P\boldsymbol{Z}_{xx}^N + \boldsymbol{Z}_{xx}^P\left(\boldsymbol{Z}_{xx}^0 + 3\boldsymbol{Z}_f\right) + \boldsymbol{Z}_{xx}^N\left(\boldsymbol{Z}_{xx}^0 + 3\boldsymbol{Z}_f\right)} \quad (17c)$$

The nodal voltages can be calculated by means of sequence currents and the transfer impedances in the corresponding sequence. The positive-sequence voltage is the only sequence voltage that is present prior to the fault and is equal to the pre-fault voltage at phase *a*. Thus, the during fault sequence voltages are

$$\boldsymbol{V}^{P,mx} = \boldsymbol{V}_a^{pref(m)} - \boldsymbol{Z}_{mx}^P \frac{\boldsymbol{V}_a^{pref(x)}\left(\boldsymbol{Z}_{xx}^N + \boldsymbol{Z}_{xx}^0 + 3\boldsymbol{Z}_f\right)}{\boldsymbol{Z}_{xx}^P\boldsymbol{Z}_{xx}^N + \boldsymbol{Z}_{xx}^P\left(\boldsymbol{Z}_{xx}^0 + 3\boldsymbol{Z}_f\right) + \boldsymbol{Z}_{xx}^N\left(\boldsymbol{Z}_{xx}^0 + 3\boldsymbol{Z}_f\right)} \quad (18a)$$

$$\boldsymbol{V}^{N,mx} = \boldsymbol{Z}_{mx}^N \frac{\boldsymbol{V}_a^{pref(x)}\left(\boldsymbol{Z}_{xx}^0 + 3\boldsymbol{Z}_f\right)}{\boldsymbol{Z}_{xx}^P\boldsymbol{Z}_{xx}^N + \boldsymbol{Z}_{xx}^P\left(\boldsymbol{Z}_{xx}^0 + 3\boldsymbol{Z}_f\right) + \boldsymbol{Z}_{xx}^N\left(\boldsymbol{Z}_{xx}^0 + 3\boldsymbol{Z}_f\right)} \quad (18b)$$

$$\boldsymbol{V}^{0,mx} = \boldsymbol{Z}_{mx}^0 \frac{\boldsymbol{V}_a^{pref(x)}\boldsymbol{Z}_{xx}^N}{\boldsymbol{Z}_{xx}^P\boldsymbol{Z}_{xx}^N + \boldsymbol{Z}_{xx}^P\left(\boldsymbol{Z}_{xx}^0 + 3\boldsymbol{Z}_f\right) + \boldsymbol{Z}_{xx}^N\left(\boldsymbol{Z}_{xx}^0 + 3\boldsymbol{Z}_f\right)} \quad (18c)$$

Finally, the during-fault phase voltages are found by applying the symmetrical component transformation as follows

$$\boldsymbol{V}_a^{mx} = \boldsymbol{V}_a^{pref(m)} + \boldsymbol{V}_a^{pref(x)} \frac{\left\{\left(\boldsymbol{Z}_{mx}^N - \boldsymbol{Z}_{mx}^P\right)\left(\boldsymbol{Z}_{xx}^0 + 3\boldsymbol{Z}_f\right) + \left(\boldsymbol{Z}_{mx}^0 - \boldsymbol{Z}_{mx}^P\right)\boldsymbol{Z}_{xx}^N\right\}}{\boldsymbol{Z}_{xx}^P\boldsymbol{Z}_{xx}^N + \boldsymbol{Z}_{xx}^P\left(\boldsymbol{Z}_{xx}^0 + 3\boldsymbol{Z}_f\right) + \boldsymbol{Z}_{xx}^N\left(\boldsymbol{Z}_{xx}^0 + 3\boldsymbol{Z}_f\right)} \quad (19a)$$

$$\boldsymbol{V}_b^{mx} = a^2\boldsymbol{V}_a^{pref(m)} + \boldsymbol{V}_a^{pref(x)} \frac{\left\{\left(a\,\boldsymbol{Z}_{mx}^N - a^2\boldsymbol{Z}_{mx}^P\right)\left(\boldsymbol{Z}_{xx}^0 + 3\boldsymbol{Z}_f\right) + \left(\boldsymbol{Z}_{mx}^0 - a^2\boldsymbol{Z}_{mx}^P\right)\boldsymbol{Z}_{xx}^N\right\}}{\boldsymbol{Z}_{xx}^P\boldsymbol{Z}_{xx}^N + \boldsymbol{Z}_{xx}^P\left(\boldsymbol{Z}_{xx}^0 + 3\boldsymbol{Z}_f\right) + \boldsymbol{Z}_{xx}^N\left(\boldsymbol{Z}_{xx}^0 + 3\boldsymbol{Z}_f\right)} \quad (19b)$$

$$\boldsymbol{V}_c^{mx} = a\boldsymbol{V}_a^{pref(m)} + \boldsymbol{V}_a^{pref(x)} \frac{\left\{\left(a^2\boldsymbol{Z}_{mx}^N - a\,\boldsymbol{Z}_{mx}^P\right)\left(\boldsymbol{Z}_{xx}^0 + 3\boldsymbol{Z}_f\right) + \left(\boldsymbol{Z}_{mx}^0 - a\,\boldsymbol{Z}_{mx}^P\right)\boldsymbol{Z}_{xx}^N\right\}}{\boldsymbol{Z}_{xx}^P\boldsymbol{Z}_{xx}^N + \boldsymbol{Z}_{xx}^P\left(\boldsymbol{Z}_{xx}^0 + 3\boldsymbol{Z}_f\right) + \boldsymbol{Z}_{xx}^N\left(\boldsymbol{Z}_{xx}^0 + 3\boldsymbol{Z}_f\right)} \quad (19c)$$

2.3. Voltage-dip and Phase-angle Jump for four types of Dips

Four types of voltage dips may exist in electricity networks; they are A, B, E and G type. Dip-types A, B, and E are obtained due to 3-phase, single line-to-ground, and phase-to-phase faults, measured at the fault location. Dip-type G is usually found for double line-to-ground faults [26]. In summary, dip-type A is found due to severely affected *abc*-phase, dip-type B is seen due to severely affected single-phase (*a*-phase or *b*-phase or *c*-phase), whereas dip-types E and G are encountered due to severely affected double-phase (*ab*-phase or *bc*-phase or *ca*-phase) voltages. Phasor representation of four types of voltage dips with severely affected dip-phase is illustrated in Fig. 4. In the following section, the expression of voltage-dip d_v is derived for four types of dips, assuming the pre-fault voltage at monitoring bus *m* and the faulted bus *x* is $1\angle 0°$.

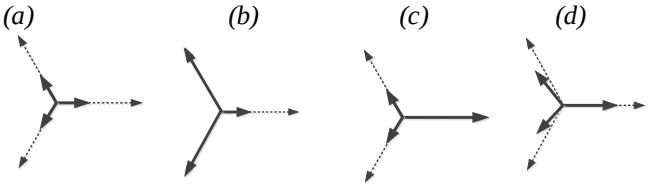

Fig. 4. *Voltage phasors for four types of voltage dips: (a) Type A, (b) Type B, (c) Type E, and (d) Type G.*

2.3.1 Voltage-dip d_v for Type A: From (6), the expression of phase-*a* magnitude for type-A dip can be given by (assuming pre-fault voltages as $1\angle 0°$)

$$\left|\boldsymbol{V}_a^{mx}\right| = \left|1 - \frac{\boldsymbol{Z}_{mx}}{\boldsymbol{Z}_{xx} + \boldsymbol{Z}_f}\right| \quad (20)$$

Thus, for dip-type A, the expression of voltage-dip d_v, observed at monitoring bus *m* due to fault at bus *x*, is given by

$$d_v^{mx} = 1 - \left|1 - \frac{\boldsymbol{Z}_{mx}}{\boldsymbol{Z}_{xx} + \boldsymbol{Z}_f}\right| \quad (21)$$

2.3.2 Voltage-dip d_v for Type B: Taking the phase-voltage *a*into account, from (13a), the expression of phase-*a* magnitude for dip-type Bcan be given by (assuming pre-fault voltages $=1\angle 0°$)

$$\left|\boldsymbol{V}_a^{mx}\right| = \left|1 - \frac{\boldsymbol{Z}_{mx}^P + \boldsymbol{Z}_{mx}^N + \boldsymbol{Z}_{mx}^0}{\boldsymbol{Z}_{xx}^P + \boldsymbol{Z}_{xx}^N + \boldsymbol{Z}_{xx}^0 + 3\boldsymbol{Z}_f}\right| \quad (22)$$

Thus, for dip-type B, the expressions of voltage-dip d_v, observed at monitoring bus *m* due to fault at bus *x*, are given by

$$d_v^{mx} = 1 - \left|1 - \frac{\boldsymbol{Z}_{mx}^P + \boldsymbol{Z}_{mx}^N + \boldsymbol{Z}_{mx}^0}{\boldsymbol{Z}_{xx}^P + \boldsymbol{Z}_{xx}^N + \boldsymbol{Z}_{xx}^0 + 3\boldsymbol{Z}_f}\right| \quad (23)$$

2.3.3 Voltage-dip d_v for Type E: Taking the phase-voltage *b* into account, from Eq. (16b), the expression of phase-*b* magnitude for dip-type E can be given by (assuming pre-fault voltages $=1\angle 0°$)

$$\left|\boldsymbol{V}_b^{mx}\right| = \left|e^{j4\pi/3} + \frac{e^{j2\pi/3}\boldsymbol{Z}_{mx}^N - e^{j4\pi/3}\boldsymbol{Z}_{mx}^P}{\boldsymbol{Z}_{xx}^P + \boldsymbol{Z}_{xx}^N + \boldsymbol{Z}_f}\right| \quad (24)$$

Thus, for dip-type E, the expressions of voltage-dip d_v, observed at monitoring bus *m* due to fault at bus *x*, are given by

$$d_v^{mx} = 1 - \left|e^{j4\pi/3} + \frac{e^{j2\pi/3}\boldsymbol{Z}_{mx}^N - e^{j4\pi/3}\boldsymbol{Z}_{mx}^P}{\boldsymbol{Z}_{xx}^P + \boldsymbol{Z}_{xx}^N + \boldsymbol{Z}_f}\right| \quad (25)$$

Table 1 Expressions of Phase-angle Jumps for different Dip-types

Dip-types	Phase-angle jump at monitoring node *m* due to fault at bus *x*
A	$\Delta\mu_a^{mx} = \left\lvert \arg\left\{ \boldsymbol{e}^{j0} - \frac{\boldsymbol{Z}_{mx}}{\boldsymbol{Z}_{xx} + \boldsymbol{Z}_f} \right\} \right\rvert = \Delta\mu_b^{mx} = \Delta\mu_c^{mx}$
B	$\Delta\mu_a^{mx} = \left\lvert \arg\left\{ \boldsymbol{e}^{j0} - \frac{\boldsymbol{Z}_{mx}^P + \boldsymbol{Z}_{mx}^N + \boldsymbol{Z}_{mx}^0}{\boldsymbol{Z}_{xx}^P + \boldsymbol{Z}_{xx}^N + \boldsymbol{Z}_{xx}^0 + 3\boldsymbol{Z}_f} \right\} \right\rvert$, $\Delta\mu_b^{mx} = \left\lvert \frac{4\pi}{3} - \arg\left\{ \boldsymbol{e}^{j4\pi/3} - \frac{\boldsymbol{e}^{j4\pi/3}\boldsymbol{Z}_{mx}^P + \boldsymbol{e}^{j2\pi/3}\boldsymbol{Z}_{mx}^N + \boldsymbol{Z}_{mx}^0}{\boldsymbol{Z}_{xx}^P + \boldsymbol{Z}_{xx}^N + \boldsymbol{Z}_{xx}^0 + 3\boldsymbol{Z}_f} \right\} \right\rvert$, $\Delta\mu_c^{mx} = \left\lvert \frac{2\pi}{3} - \arg\left\{ \boldsymbol{e}^{j2\pi/3} - \frac{\boldsymbol{e}^{j2\pi/3}\boldsymbol{Z}_{mx}^P + \boldsymbol{e}^{j4\pi/3}\boldsymbol{Z}_{mx}^N + \boldsymbol{Z}_{mx}^0}{\boldsymbol{Z}_{xx}^P + \boldsymbol{Z}_{xx}^N + \boldsymbol{Z}_{xx}^0 + 3\boldsymbol{Z}_f} \right\} \right\rvert$
E	$\Delta\mu_a^{mx} = \left\lvert \arg\left\{ \boldsymbol{e}^{j0} + \frac{\boldsymbol{Z}_{mx}^N - \boldsymbol{Z}_{mx}^P}{\boldsymbol{Z}_{xx}^P + \boldsymbol{Z}_{xx}^N + \boldsymbol{Z}_f} \right\} \right\rvert$, $\Delta\mu_b^{mx} = \left\lvert \frac{4\pi}{3} - \arg\left\{ \boldsymbol{e}^{j4\pi/3} + \frac{\boldsymbol{e}^{j2\pi/3}\boldsymbol{Z}_{mx}^N - \boldsymbol{e}^{j4\pi/3}\boldsymbol{Z}_{mx}^P}{\boldsymbol{Z}_{xx}^P + \boldsymbol{Z}_{xx}^N + \boldsymbol{Z}_f} \right\} \right\rvert$, $\Delta\mu_c^{mx} = \left\lvert \frac{2\pi}{3} - \arg\left\{ \boldsymbol{e}^{j2\pi/3} + \frac{\boldsymbol{e}^{j4\pi/3}\boldsymbol{Z}_{mx}^N - \boldsymbol{e}^{j2\pi/3}\boldsymbol{Z}_{mx}^P}{\boldsymbol{Z}_{xx}^P + \boldsymbol{Z}_{xx}^N + \boldsymbol{Z}_f} \right\} \right\rvert$
G	$\mu_a^{mx} = \left\lvert \arg\left[\boldsymbol{e}^{j0} + \frac{\left\{ \left(\boldsymbol{Z}_{mx}^N - \boldsymbol{Z}_{mx}^P\right)\left(\boldsymbol{Z}_{xx}^0 + 3\boldsymbol{Z}_f\right) + \left(\boldsymbol{Z}_{mx}^0 - \boldsymbol{Z}_{mx}^P\right)\boldsymbol{Z}_{xx}^N \right\}}{\boldsymbol{Z}_{xx}^P\boldsymbol{Z}_{xx}^N + \boldsymbol{Z}_{xx}^P\left(\boldsymbol{Z}_{xx}^0 + 3\boldsymbol{Z}_f\right) + \boldsymbol{Z}_{xx}^N\left(\boldsymbol{Z}_{xx}^0 + 3\boldsymbol{Z}_f\right)} \right] \right\rvert$
	$\Delta\mu_b^{mx} = \left\lvert \frac{4\pi}{3} - \arg\left[\boldsymbol{e}^{j4\pi/3} + \frac{\left\{ \left(\boldsymbol{e}^{j2\pi/3}\boldsymbol{Z}_{mx}^N - \boldsymbol{e}^{j4\pi/3}\boldsymbol{Z}_{mx}^P\right)\left(\boldsymbol{Z}_{xx}^0 + 3\boldsymbol{Z}_f\right) + \left(\boldsymbol{Z}_{mx}^0 - \boldsymbol{e}^{j4\pi/3}\boldsymbol{Z}_{mx}^P\right)\boldsymbol{Z}_{xx}^N \right\}}{\boldsymbol{Z}_{xx}^P\boldsymbol{Z}_{xx}^N + \boldsymbol{Z}_{xx}^P\left(\boldsymbol{Z}_{xx}^0 + 3\boldsymbol{Z}_f\right) + \boldsymbol{Z}_{xx}^N\left(\boldsymbol{Z}_{xx}^0 + 3\boldsymbol{Z}_f\right)} \right] \right\rvert$
	$\Delta\mu_c^{mx} = \left\lvert \frac{2\pi}{3} - \arg\left[\boldsymbol{e}^{j2\pi/3} + \frac{\left\{ \left(\boldsymbol{e}^{j4\pi/3}\boldsymbol{Z}_{mx}^N - \boldsymbol{e}^{j2\pi/3}\boldsymbol{Z}_{mx}^P\right)\left(\boldsymbol{Z}_{xx}^0 + 3\boldsymbol{Z}_f\right) + \left(\boldsymbol{Z}_{mx}^0 - \boldsymbol{e}^{j2\pi/3}\boldsymbol{Z}_{mx}^P\right)\boldsymbol{Z}_{xx}^N \right\}}{\boldsymbol{Z}_{xx}^P\boldsymbol{Z}_{xx}^N + \boldsymbol{Z}_{xx}^P\left(\boldsymbol{Z}_{xx}^0 + 3\boldsymbol{Z}_f\right) + \boldsymbol{Z}_{xx}^N\left(\boldsymbol{Z}_{xx}^0 + 3\boldsymbol{Z}_f\right)} \right] \right\rvert$

2.3.4 Voltage-dip d_v for Type G: Considering the phase-voltage *b*,from Eq. (19b), the expression of phase-*b* magnitude for dip-type G can be given by (assuming pre-fault voltages $=1\angle 0°$)

$$\left|\boldsymbol{V}_b^{mx}\right| = \left| \begin{array}{l} \boldsymbol{e}^{j4\pi/3} + \\ \frac{\left\{ \left(\boldsymbol{e}^{j2\pi/3}\boldsymbol{Z}_{mx}^N - \boldsymbol{e}^{j4\pi/3}\boldsymbol{Z}_{mx}^P\right)\left(\boldsymbol{Z}_{xx}^0 + 3\boldsymbol{Z}_f\right) \right\}}{\boldsymbol{Z}_{xx}^P\boldsymbol{Z}_{xx}^N + \boldsymbol{Z}_{xx}^P\left(\boldsymbol{Z}_{xx}^0 + 3\boldsymbol{Z}_f\right) + \boldsymbol{Z}_{xx}^N\left(\boldsymbol{Z}_{xx}^0 + 3\boldsymbol{Z}_f\right)} + \\ \frac{\left\{ \left(\boldsymbol{Z}_{mx}^0 - \boldsymbol{e}^{j4\pi/3}\boldsymbol{Z}_{mx}^P\right)\boldsymbol{Z}_{xx}^N \right\}}{\boldsymbol{Z}_{xx}^P\boldsymbol{Z}_{xx}^N + \boldsymbol{Z}_{xx}^P\left(\boldsymbol{Z}_{xx}^0 + 3\boldsymbol{Z}_f\right) + \boldsymbol{Z}_{xx}^N\left(\boldsymbol{Z}_{xx}^0 + 3\boldsymbol{Z}_f\right)} \end{array} \right| \quad (26)$$

Thus, for dip-type G, the expressions of voltage-dip d_v, observed at monitoring bus *m* due to fault at bus *x*, are given by

$$d_v^{mx} = 1 - \left|\Omega_G\right| \quad (27)$$

where $\Omega_G = \boldsymbol{e}^{j4\pi/3} + \frac{\left\{ \left(\boldsymbol{e}^{j2\pi/3}\boldsymbol{Z}_{mx}^N - \boldsymbol{e}^{j4\pi/3}\boldsymbol{Z}_{mx}^P\right)\left(\boldsymbol{Z}_{xx}^0 + 3\boldsymbol{Z}_f\right) \right\}}{\boldsymbol{Z}_{xx}^P\boldsymbol{Z}_{xx}^N + \boldsymbol{Z}_{xx}^P\left(\boldsymbol{Z}_{xx}^0 + 3\boldsymbol{Z}_f\right) + \boldsymbol{Z}_{xx}^N\left(\boldsymbol{Z}_{xx}^0 + 3\boldsymbol{Z}_f\right)} + \frac{\left\{ \left(\boldsymbol{Z}_{mx}^0 - \boldsymbol{e}^{j4\pi/3}\boldsymbol{Z}_{mx}^P\right)\boldsymbol{Z}_{xx}^N \right\}}{\boldsymbol{Z}_{xx}^P\boldsymbol{Z}_{xx}^N + \boldsymbol{Z}_{xx}^P\left(\boldsymbol{Z}_{xx}^0 + 3\boldsymbol{Z}_f\right) + \boldsymbol{Z}_{xx}^N\left(\boldsymbol{Z}_{xx}^0 + 3\boldsymbol{Z}_f\right)}$

The expressions of $d_v$for four types of dips are presented in Eqs. (21), (23), (25) and (27). Along with the reduction of the voltage magnitude, as presented through the expressions of d_v^{mx}, remote fault also leads to a variation in the phase angle of the voltage. This variation of phase angle is known as phase-angle jump [27]. From Eq. (6) it can be observed that for symmetrical fault or type-A dip, phase-angle jump occurs when the quotient $\boldsymbol{Z}_{mx}/(\boldsymbol{Z}_{xx} + \boldsymbol{Z}_f)$ is not a real number. However, for unsymmetrical fault or dip-types B, E and G, the phase-angle jump of each phase-voltage are considered separately. From expressions (3)-(19), the phase-angle jumps corresponding to four types of voltage dips can be easily derived, and these are given in Table 1. Note that for deriving the expressions of phase-angle jump, pre-fault voltage is assumed to be $1\angle 0°$. Moreover, due to fault at bus *x* and monitoring point at bus *m* of Fig. 1, the phase-angle jumps at *a*-, *b*-, and *c*-phase are denoted as $\Delta\mu_a^{mx}$, $\Delta\mu_b^{mx}$, and $\Delta\mu_c^{mx}$, respectively.

3. Illustrative Example for validating the Analytical Expressions of Voltage Dips

In Section 3.1, a simulation study is conducted which explores different types of dips and their associated phase-angle jumps at different buses during different types of faults. Then, in Section 3.2, validation of the analytical expressions of Section 2 is carried out considering the common test system and experimental platform.

3.1. Simulation Study

Single line diagram of a simple radial distribution network is shown in Fig. 5. This test system is simulated using MATLAB/SIMPOWER softwareto analyse the different types of fault-initiated dips at different buses of the system. The upstream side of the test system is represented by Thévenin equivalent of the utility grid, where voltage level and fault level are considered as 66 kV and 1000 MVA, respectively. It is connected to PCC busthrough a 66/11 kV transformer. Three-phase loads aredistributed along the distribution feeder.

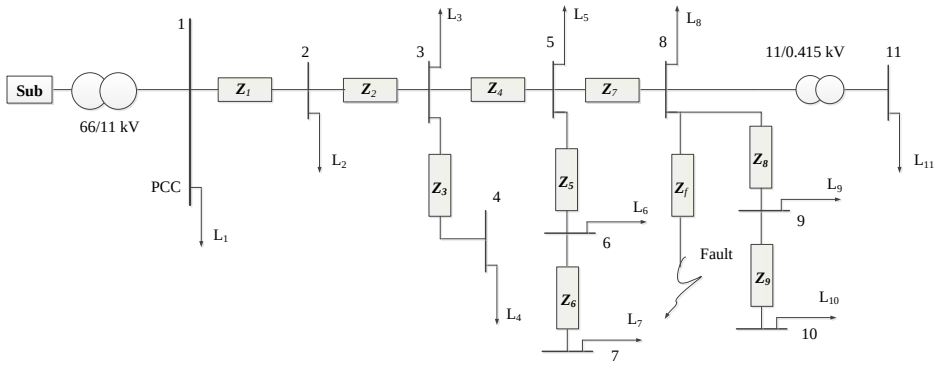

Fig. 5. *Single line diagram of a radial distribution network.*

Now, due to fault at any arbitrary bus(for this study, bus 8 is selected), voltages and their corresponding phase-angle at different buses are monitored. As discussed in section 2, four types of faults are usually found in power system; they are Single line-to-ground (SLG) fault, phase-to-phase fault, double line-to-ground fault and symmetrical or balanced 3-phase fault. These faults are the primary reason for developing different types of dips. However, propagation of dips through different network elements can change the type of dips. For example, transformer winding connection and load-connection can influence the type of dips, which are presented in Sections 3.1.1 and 3.1.2, respectively.

3.1.1Transformer Winding Connection: Transformer winding connections are classified into three types to explain the transfer of three-phase unbalanced voltage dips, as well as the change in voltage dip-type, from one voltage level to another [4].

- Type 1 – Transformers that do not change anything to the voltages. The primary voltages (per unit) are equal to the secondary per unit voltages. The only transformer configuration that falls under this type is the Wye Grounded-Wye grounded (Yg-Yg).
- Type 2 – Transformers that remove the zero-sequence voltage. Basically, the secondary voltage (pu) is equal to the primary voltage (pu) minus the zero-sequence component. The Delta-delta (Dd), Delta-zigzag (Dz) and the Wye-wye (with both windings ungrounded or with only one star point grounded) belong to this type.
- Type 3 – Transformers that changes line and phase voltages. Delta-wye (Dy), Wye-delta (Yd) and the Wye-zigzag (Yz) fit under this type.

3.1.2Load Connection: Three-phase loads in power networks are usually connected in two ways: wye-connected and delta-connected. These types of connectivity of loads, along with different combinations of fault-types and transformer-types, can also influence the type of dips. In the simulation study, the four types of dips, as discussed in Section 2.3, are generated by using the combinations of three factors, i.e., fault-type, winding connection of transformer, and load-connection. The combinations, which have been applied for generating the four types of dips, are shown in Table 2.

Table 3 illustrates the voltage-dip (d_v) and phase-angle jumps associated with four types of dips. These dips are encountered at bus 10 of Fig. 5, due to fault at bus 8. To demonstrate the effect of voltage-dip and phase-angle jump, Fig. 6 illustrates the instantaneous 3-phase voltages, their associated phase-angle, voltage-dip (d_v) for type-B dip with severely affected *a*-phase. In addition, to investigate the effect of voltage-dip and phase-angle jumps at all other buses in the distribution feeder, a SLG and phase-to-phase fault-initiated B- and E-types dips are simulated, and the results are illustrated in Table4. Like the previous analysis as conducted for monitoring bus 10, the other buses also encounter the difference in voltage-dip (d_v) and phase-angle jumps. However, buses in the proximity of fault encounter larger voltage-dip in comparison to the buses at farther away from the fault-point.

Table 2 Generation of Four Types of Dips considering different combinations of Network Elements and Faults [4]

Dip-type	Fault-type	Transformer type			Load Connection	
		Type 1: Yg-Yg	Type 2: Dd	Type 3: Dy	Wye	Delta
A	3Φ	No effect on transformer type			No effect on load connection	
B	LG	Yes			Yes	
E	LLG	Yes			Yes	
G	LLG		Yes	Yes	Yes	Yes

Table 3 Four Types of Voltage Dips observed at bus 10

Voltage Dip-type	Ground-truth (Severely affected dip-phase)	Voltage – Dip (d_v)	Phase-angle jump		
			$\lvert\Delta\mu_a\rvert°$	$\lvert\Delta\mu_b\rvert°$	$\lvert\Delta\mu_c\rvert°$
A	*abc*-phase	0.9212	65.37	65.37	65.37
B	*a*-phase	0.9488	68.75	15.14	13.59
E	*ab*-phase	0.4777	58.91	58.74	0
G	*ab*-phase	0.9607	2	68.74	7

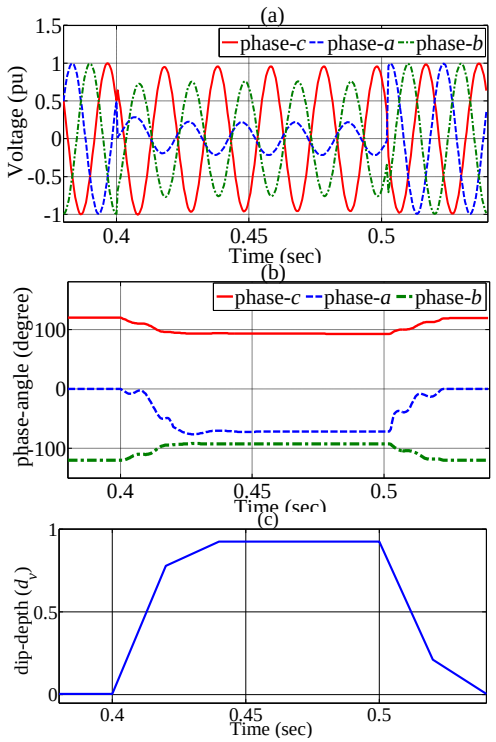

Fig. 6. *(a) Instantaneous 3-phase voltages, (b) its phase-angles in time-domain, and (c) the associated voltage-dip (d_v), observed at bus 10 due to voltage dip B-type with severely affected a-phase.*

3.2. Validation of Analytical Expressions of Voltage Dips

In Section 3.1, the voltage-dip (d_v) and phase-angle jumps under different types of faults are calculated using the simulated results at different monitoring buses. To validate the expressions developed in Section 2, this sub-section explores the case by case study of different types of fault-initiated dips and their associated phase-angle jumps employing the developed analytical expressions as well as through network simulations. To this end, voltage-dips and phase-angle jumps, as observed at buses 1-11 due to fault at bus 8, are calculated from the impedance matrix of the test network shown in Fig. 5 and the analytical expressions associated with balanced and unbalanced faults. The results can be seen in Table 5. Note that the proposed analytical expressions are developed in a MATLAB script, which is executed to characterise the fault-initiated voltage dips and phase angle jumps at different buses.To carry out the validation, the results obtained through simulation and analytical expressions are placed side by side. Less than 1% difference is found in the test results, which indicate the acceptability of the developed expressions of Section 2.

To conduct the further validation of the developed expressions, balanced 3-phase faults are considered. The during-fault bus voltages and phase-angle jumps at all buses in the distribution feeder are observed. The voltage-dip (d_v) at different buses obtained through simulations and analytical expressions are shown in Fig. 7(a), whereas the phase-angle jumps obtained through analytical expressions and simulations are highlighted in Fig. 7(b). Following the similar approach, unbalanced faults, such as, SLG and phase-to-phase faultsare investigated.Negligible difference between expressions and simulation results is found in all the test cases, which is in line with the previous study; see Table 6 for illustration.

Table 4 Voltage Dips and Phase-angle Jumps Observed at different buses due to SLG and LLG Fault at bus 8

Voltage Dip-type	Bus Number	Voltage – Dip (d_v)	Phase-angle jump		
			$\lvert\Delta\mu_a\rvert^\circ$	$\lvert\Delta\mu_b\rvert^\circ$	$\lvert\Delta\mu_c\rvert^\circ$
B	1	0.059	1.42	1.44	1.86
B	2	0.108	2.59	1.44	1.86
B	3	0.4015	4.11	5.20	4.10
B	4	0.4015	4.11	5.20	4.10
B	5	0.6966	8.43	10.52	9.18
B	6	0.6966	8.43	10.52	9.18
B	7	0.6966	8.43	10.52	9.18
B	8	0.9488	68.75	15.14	13.59
B	9	0.9488	68.75	15.14	13.59
B	10	0.9488	68.75	15.14	13.59
B	11	0.9488	68.75	15.14	13.59
E	1	0.0912	0	5.77	1.80
E	2	0.1334	0	9.30	3.20
E	3	0.2977	0	20.24	14.73
E	4	0.2977	0	20.24	14.73
E	5	0.4221	0	36.67	33.08
E	6	0.4221	0	36.67	33.08
E	7	0.4221	0	36.67	33.08
E	8	0.4777	0	58.91	58.74
E	9	0.4777	0	58.91	58.74
E	10	0.4777	0	58.91	58.74
E	11	0.4777	0	58.91	58.74

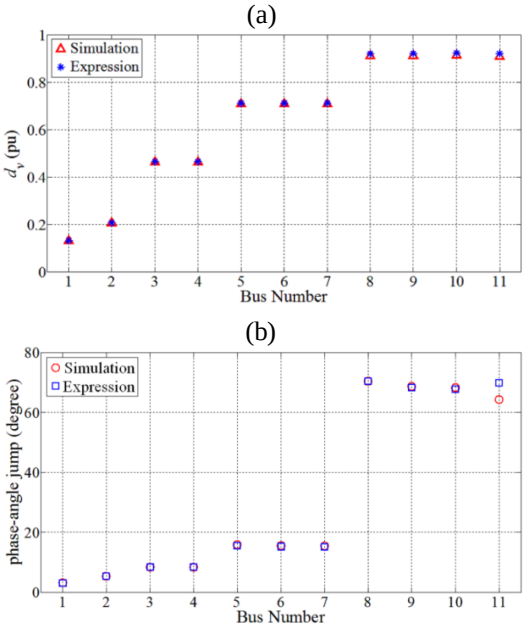

Fig. 7. *Voltage-dip (d_v) and phase-angle jumps at differentbuses due to balanced 3-phase faults at bus 8:* ***(a)*** *$d_v$obtained from analytical expression and simulation;* ***(b)****phase-angle jumps obtained from analytical expression and simulation.*

Table 5 Voltage Dips, Phase-angle Jumps at Bus 10 obtained through Analytical Expression and Simulation due to Fault at Bus 8

Voltage Dip-types	Ground-truth (Severely affected dip-phase)	Analytical expression				Simulation			
		Voltage-dip (d_v)	Phase-angle jump			Voltage-dip (d_v)	Phase-angle jump		
			$\lvert\Delta\mu_a\rvert^\circ$	$\lvert\Delta\mu_b\rvert^\circ$	$\lvert\Delta\mu_c\rvert^\circ$		$\lvert\Delta\mu_a\rvert^\circ$	$\lvert\Delta\mu_b\rvert^\circ$	$\lvert\Delta\mu_c\rvert^\circ$
A	*abc*-phase	0.924	67.77	67.77	67.77	0.9212	65.37	65.37	65.37
B	*a*-phase	0.9478	68.72	14.85	13.51	0.9488	68.75	15.14	13.59
E	*bc*-phase	0.4667	0	58.89	58.73	0.4777	0	58.91	58.74
G	*bc*-phase	0.9597	3	69	6	0.9607	2	68.74	7

Table 6 Voltage Dips and Phase-angle Jumps at different buses obtained through Analytical Expression and Simulation due to Fault at Bus 8

Fault Type	Voltage Dip-types	Bus Number	Analytical expression				Simulation			
			Voltage-dip (d_v)	Phase-angle jump			Voltage-dip (d_v)	Phase-angle jump		
				$\lvert\Delta\mu_a\rvert^\circ$	$\lvert\Delta\mu_b\rvert^\circ$	$\lvert\Delta\mu_c\rvert^\circ$		$\lvert\Delta\mu_a\rvert^\circ$	$\lvert\Delta\mu_b\rvert^\circ$	$\lvert\Delta\mu_c\rvert^\circ$
SLG	B	1	0.0581	1.38	1.15	1.78	0.059	1.42	1.44	1.86
	B	2	0.1069	2.56	1.15	1.78	0.108	2.59	1.44	1.86
	B	3	0.3974	4.07	4.91	4.02	0.4015	4.11	5.20	4.10
	B	4	0.3974	4.07	4.91	4.02	0.4015	4.11	5.20	4.10
	B	5	0.6866	8.39	10.23	9.10	0.6966	8.43	10.52	9.18
	B	6	0.6866	8.39	10.23	9.10	0.6966	8.43	10.52	9.18
	B	7	0.6866	8.39	10.23	9.10	0.6966	8.43	10.52	9.18
	B	8	0.9478	68.72	14.85	13.51	0.9488	68.75	15.14	13.59
	B	9	0.9478	68.72	14.85	13.51	0.9488	68.75	15.14	13.59
	B	10	0.9478	68.72	14.85	13.51	0.9488	68.75	15.14	13.59
	B	11	0.9478	68.72	14.85	13.51	0.9488	68.75	15.14	13.59
Phase-to-phase	E	1	0.0802	0	5.74	1.79	0.0912	0	5.77	1.80
	E	2	0.1224	0	9.27	3.19	0.1334	0	9.30	3.20
	E	3	0.2867	0	20.22	14.72	0.2977	0	20.24	14.73
	E	4	0.2867	0	20.22	14.72	0.2977	0	20.24	14.73
	E	5	0.4111	0	36.65	33.07	0.4221	0	36.67	33.08
	E	6	0.4111	0	36.65	33.07	0.4221	0	36.67	33.08
	E	7	0.4111	0	36.65	33.07	0.4221	0	36.67	33.08
	E	8	0.4667	0	58.89	58.73	0.4777	0	58.91	58.74
	E	9	0.4667	0	58.89	58.73	0.4777	0	58.91	58.74
	E	10	0.4667	0	58.89	58.73	0.4777	0	58.91	58.74
	E	11	0.4667	0	58.89	58.73	0.4777	0	58.91	58.74

Table 7 Voltage Dips and Phase-angle Jumps at different buses for different Fault-types

Faulted Bus	Monitoring Bus	Fault-types							
		Balanced 3-phase fault		SLG Fault		LL fault		LLG fault	
		Voltage-dip (d_v)	Phase-angle Jump (degree)	Voltage -dip (d_v)	Phase-angle Jump (degree)	Voltage-dip (d_v)	Phase-angle Jump (degree)	Voltage -dip (d_v)	Phase-angle Jump (degree)
8	1	0.1314	3.12	0.0575	1.38	0.0797	5.77	0.0947	6.11
	2	0.2067	5.33	0.106	2.56	0.1215	9.31	0.1567	10.31
	3	0.4624	8.36	0.3964	4.26	0.285	20.30	0.4445	22.30
	4	0.4626	8.37	0.3964	4.26	0.285	20.30	0.4445	22.30
	5	0.7088	15.87	0.6853	9.07	0.4082	36.74	0.7315	38.94
	6	0.7084	15.55	0.6853	9.07	0.4082	36.74	0.7315	38.94
	7	0.7085	15.45	0.6853	9.07	0.4082	36.74	0.7315	38.94
	8	0.9118	70.42	0.9422	70.18	0.4625	58.86	0.9577	59.86
	9	0.9138	68.66	0.9422	70.18	0.4625	58.86	0.9577	59.86
	10	0.9147	68.24	0.9422	70.18	0.4625	58.86	0.9577	59.86
	11	0.9093	64.28	0.9401	64.65	0.4623	57.95	0.9644	56.95

The validation of the developed analytical expressions are also conducted by comparing the resultswith the real-time simulation study inMATLAB/SIMPOWER and OPAL-RT simulation platform. To this end, a SLG (*a*-phase-to-ground) anda phase-to-phase (*b*-phase-to-*c*-phase)faults are simulated in real-time at bus 5 and bus 9, respectively, using the test system of Fig. 5.Then, the voltage-dip (d_v)and phase-angle jump ($|\Delta\mu_a|$ for SLG and $|\Delta\mu_b|$ for phase-to-phase fault) at all buses are obtained. The results (voltage-dip and phase-angle jump at different buses) are illustrated in Figs. 8 and 9. Negligible differences are observedbetween the results obtained from real-time simulation study and analytical expressions, see Figs. 8 and 9 for illustration.

(a)(b)

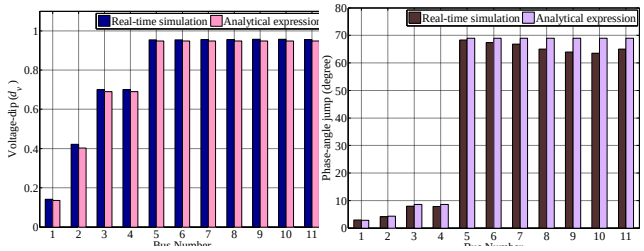

Fig. 8. *Voltage-dip (d_v) and phase-angle jumps at differentbuses due to singleline-to-ground (SLG) fault at bus 5:*
(a) *d_v (pu) obtained from analytical expression and real-time simulation;*
(b) *phase-angle jump$|\Delta\mu_a|$ obtained from analytical expression and real-time simulation.*

(a)

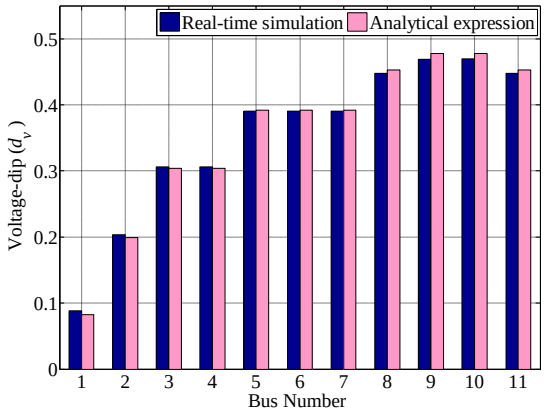

(b)

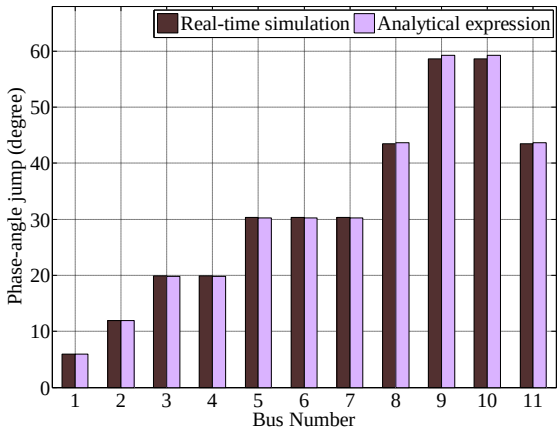

Fig. 9. *Voltage-dip (d_v) and phase-angle jumps at different buses due to phase-to-phase fault at bus 9:*
(a) *d_v(pu) obtained from analytical expression and real-time simulation;*
(b) *phase-angle jump$|\Delta\mu_b|$ obtained from analytical expression and real-time simulation.*

Table 8 Voltage Dips and Phase-angle Jumps at different buses due to Fault at different Location

Fault- type	Monitoring Bus	Fault location					
		Bus 1		Bus 5		Bus 8	
		Voltage-dip (d_v)	Phase-angle Jump (degree)	Voltage-dip (d_v)	Phase-angle Jump (degree)	Voltage -dip (d_v)	Phase-angle Jump (degree)
SLG	1	0.4136	54.07	0.0807	2.02	0.0575	1.38
	2	0.4007	42.18	0.1485	3.84	0.106	2.56
	3	0.3906	40.54	0.5563	8.50	0.3964	4.26
	4	0.3906	40.54	0.5563	8.50	0.3964	4.26
	5	0.38	38.96	0.9209	69.29	0.6853	9.07
	6	0.38	38.96	0.9209	69.29	0.6853	9.07
	7	0.38	38.96	0.9209	69.29	0.6853	9.07
	8	0.3689	37.44	0.8991	54.84	0.9422	70.18
	9	0.3689	37.44	0.8991	54.84	0.9422	70.18
	10	0.3689	37.44	0.8991	54.84	0.9422	70.18
	11	0.3671	36.90	0.896	52.01	0.9401	64.65

4. Characterisation of Voltage Dips

In this section, voltage dips are characterised by analysing the voltage-dip and phase-angle jumps at different buses under several scenarios, which include the fault-type, fault location and different monitoring point along the distribution feeder.

4.1. Voltage Dip Characterisation for different Fault-types

Four types of faults, as discussed earlier, are analysed using the test network of Fig. 5. Voltage-dip (d_v) and phase-angle jumps at different buses are observed due to fault at bus 8. The analytical expressions derived in Section 2 are used for this dip-observation. The results are shown in Table 7. It is to be noted that phase-angle jumps of one phase voltage, which shows the highest value, is presented in the Table 7 for different types of faults. However, the phase-angle jumps of other phase-voltages are also obtained from the network using developed expressions. From the test results it is evident that balanced 3-phase faults yield the higher $d_v$than phase-to-phase faults. SLG faults result in higher d_v than balanced 3-phase faults in the vicinity of fault location (i.e. adjacent to bus 8). Moreover, double line-to-ground faults show less $d_v$than balanced 3-phase faults at monitoring bus 1 to 4, i.e., close to the upstream side.

4.2. Voltage Dip Characterisation for different Fault-location

In this study, fault locations are selected at bus 1, 5 and 8, and the associated voltage dips, phase-angle jumps are monitored at all buses; see Table 8 for illustration. It should be noted that SLG fault is considered in this study, since 70% (approximately) of the faults in the power system are SLG-types [25]. Voltage-dips (d_v) near faults show the highest value. For instance, when fault occurs at bus 5, then phase-voltages at bus 5 and its adjacent buses, which are bus 6 and 7, experience the most severe dip as shown in Table 8. However, fault occurred adjacent to upstream bus has less severe voltage dips. For example, when fault occurs at bus 1, which is nearest to the upstream side, then voltage-dip at a monitoring bus 4 experiences less dip in comparison to the fault that occurs at bus 8 located far away from upstream grid, see Table 8 for more details.

5. Conclusion

This paper mainly investigates the voltage dips and its associated phase-angle jumps in power network due to four major types of faults, which include single line-to-ground (SLG), double line-to-ground, line-to-line or phase-to-phase and balanced 3-phase faults. Four types of voltage dips, namely, A, B, E and G, which are associated with these four types of faults, are analysed. Firstly, analytical expressions of four types of voltage-dip and their phase-angle jumps are developed. Then, a simulation study is conducted to validate the developed expressions. Simulation study demonstrates the acceptability of the developed expressions for investigating during-fault voltage dips at different buses in electricity network. Lastly, characterisation of voltage dip is also conducted under the influence of fault-types, fault-location and different observation point.

6. Acknowledgements

The authors would like to thank the support of National Renewable Energy Laboratory (NREL), Golden CO, USA, for providing the OPAL-RT real-time simulation platform.

7. References

[1] Panigrahi, B., Pandi, V. R.: 'Optimal feature selection for classification of power quality disturbances using wavelet packet-based fuzzy k-nearest neighbour algorithm', IET generation, transmission & distribution,2009, 3, (3), pp. 296-306

[2]IEEE P1250/D13 January 2011, 'IEEE guide for identifying and improving voltage quality in power systems' (IEEE, 2011), pp. 1-68

[3] McGranaghan, M.F., Mueller, D. R., Samotyj, M. J.: 'Voltage sags in industrial systems', IEEE Trans. on industry applications, 1993, 29, (2), pp. 397-403

[4] Bollen, M. H.: ' Understanding power quality problems: voltage sags and interruptions', Vol. 445 (New York: IEEE Press, 2000)

[5] Zhang, L., Bollen, M. H.: 'Characteristic of voltage dips (sags) in power systems', IEEE Trans. on power delivery, 2000, 15, (2), pp. 827-832

[6] Bhattacharyya, S., Cobben, S., Kling, W.: 'Proposal for defining voltage dip-related responsibility sharing at a point of connection', IET generation, transmission & distribution, 2012, 6, (7), pp. 619-626

[7] Wang, J., Chen, S., Lie, T. T.: 'A systematic approach for evaluating economic impact of voltage dips', Electric Power Systems Research, 2007, 77, (2), pp. 145–154

[8] Andersson, T., Nilsson, D.: 'Test and Evaluation of Voltage Dip Immunity'. Master's thesis, Chalmers University of Technology, Department of Electric Power Engineering, Gothenburg (Sweden), 2002

[9] IEEE Std 1346-1998: 'Recommended practice for evaluating electric power system compatibility with electronic process equipment', 1998

[10] Langella, R., Manco, T., Testa, A.: 'Unifying supply reliability and voltage quality in the representation of an electrical system node', 2010, IEEE Trans. on power delivery, 25, (2), pp. 1172-1181

[11] Park, C. H., Jang, G.: 'Stochastic estimation of voltage sags in a large meshed network', IEEE Trans. on power delivery, 2007, 22, (3), pp. 1655-1664

[12] Juarez, E. E., Hernandez, A.: 'An analytical approach for stochastic assessment of balanced and unbalanced voltage sags in large systems', IEEE Trans. on power delivery, 2006, 21, (3), pp. 1493-1500

[13] Bollen, M. H. J., Wang, P., Jenkins, N.: 'Analysis and consequences of the phase angle associated with a voltage sag'. Proc. Conf. Rec. Power systems Computation conf., Dresden, Germany, Aug.1996, pp. 316-322

[14] Juarez, E. E., Hernandez, A.: 'Stochastic Assessment of Phase-Angle Jumps Caused by Voltage Sags Applying an Analytical Method'. Proc. IEEE Int. Conf. on Probabilistic Methods Applied to Power Systems, Stockholm, Sweden,June 2006, pp. 1-6

[15] Alam, M. R., Muttaqi, K. M., Bouzerdoum, A.: 'A new approach for classification and characterization of voltage dips and swells using 3-d polarization ellipse parameters', IEEE Trans. on power delivery, 2015, 30, (3), pp. 1344-1353

[16] García-Sánchez, T., Gómez-Lázaro, E., Muljadi, E., Kessler, M., Molina-García, A.: 'Approach to fitting parameters and clustering for characterising measured voltage dips based on two-dimensional polarisation ellipses', IET Renewable Power Generation, 2017, 11, (10), pp. 1335-1343

[17] Bagheri, A., Gu, I., Bollen, M., Balouji, E.: 'A Robust Transform-Domain Deep Convolutional Network for Voltage Dip Classification', IEEE Trans. on power delivery, 2018

[18] García-Sánchez, T., Gómez-Lázaro, E., Muljadi, E., Kessler, M., Muñoz-Benavente, I., Molina-García, A.: 'Identification of linearised RMS-voltage dip patterns based on clustering in renewable plants', IET generation, transmission & distribution, 2017, 12, (6), pp. 1256-1262

[19] Moschitta, A., Carbone, P., Muscas, C.: 'Performance comparison of advanced techniques for voltage dip detection', IEEE Transactions on Instrumentation and Measurement, 2012, 61, (5), pp. 1494-1502

[20] Weldemariam, L., Cuk, V., Cobben, S., van Waes, J.: 'Regulation and classification of voltage dips', CIRED-Open Access Proceedings Journal, 2017, (1), pp. 832-836

[21] Chia, M. H., Khambadkone, A. M.: 'Sub-cycle Voltage Dip Classification using Matrix Pencil Method with Ellipse Fit Algorithm', IEEE Trans. on industry applications, 2015, 51, (2), pp. 1660-1668

[22]Lovisolo, L., Neto, J. M., Figueiredo, K., de Menezes Laporte, L., dos Santos Rocha, J. C.: 'Location of faults generating short-duration voltage variations in distribution systems regions from records captured at one point and decomposed into damped sinusoids', IET Generation, Transmission & Distribution, 2012, *6*, (12), pp. 1225-1234

[23] Brown, H. E.: 'Solution of large networks by matrix methods' (New York et al. Wiley, 1985)

[24] Stevenson, W. D.: 'Elements of power system analysis', 1975

[25]Das, J. C.: 'Power system analysis: short-circuit load flow and harmonics' (CRC press, 2016)

[26] Ignatova, V., Granjon, P., Bacha, S.: 'Space vector method for voltage dips and swells analysis', IEEE Trans. on power delivery, 2009, 24, (4), pp. 2054-2061

[27] Bollen, M. H.: 'Fast assessment methods for voltage sags in distribution systems', IEEE Trans. on industry applications, 1996, 32, (6), pp. 1414-1423